Approach to fully decomposing an optical force into conservative and nonconservative components

Xinning Yu,[1,4,*] Yikun Jiang,[1,4] Huajin Chen,[1,2] Shiyang Liu,[3] and Zhifang Lin[1,4,†]

[1]*State Key Laboratory of Surface Physics (SKLSP), Key Laboratory of Micro and Nano Photonic Structures (Ministry of Education), and Department of Physics, Fudan University, Shanghai 200433, China*

[2]*School of Electrical and Information Engineering, Guangxi University of Science and Technology, Liuzhou, Guangxi 545006, China*

[3]*Institute of Information Optics, Zhejiang Normal University, Jinhua, Zhejiang 321004, China*

[4]*Collaborative Innovation Center of Advanced Microstructures, Nanjing University, Nanjing 210093, China*

(Received 24 May 2019; published 16 September 2019)

One of the theoretical challenges in studying optical trapping is the decomposition of the optical force into the gradient force (conservative component) and scattering force (nonconservative component), which can be achieved either for Raleigh particles or for very large particles in the regime of ray optics. However, for the moderate particles in between these two limits, the scenario is still a mystery. In this paper we present a theoretical approach to bridge this gap and fully split the optical force acting on a spherical particle immersed in a generic monochromatic free-space optical field into two such essentially different components, which is efficient even for large particles with the exact consideration of light polarization, thus offering a benchmark for examining the effective range for application of ray optics. Our approach models general optical fields by a series of homogeneous plane waves. The analytical expressions for the gradient and scattering parts of the optical force exerted on a spherical particle of arbitrary size illuminated by multiple interferential plane waves are then derived. As examples of applications, we investigate the gradient and scattering forces acting on a dielectric particle immersed in the Bessel beam. Our results are in excellent agreement with those obtained based on ray optics methods when the illuminated particle is large enough, while exhibiting effects of Mie resonance that are totally missing in the ray optics for moderate particle sizes. Finally, we study the effect of particle size on the gradient force acting on a spherical particle sitting in multiple interferential plane waves. Our extensively numerical results, up to a size as large as 2000 illuminating wavelengths, suggest an overall decreasing tendency in the ratio of the magnitude of the gradient force to that of the total force as the particle size increases.

DOI: 10.1103/PhysRevA.100.033821

I. INTRODUCTION

Optical micromanipulation, pioneered by Ashkin [1,2], has attracted much attention during the past several decades. Up to now optical micromanipulation is widely used in the fields of biology, physical chemistry, and physics [3–6]. Decomposing the optical force into conservative and nonconservative components is one of the general problems of paramount importance, since these two components play essentially different roles in optical micromanipulation [7,8]. The customary decomposition of optical force can be expressed by $\mathbf{F} = \mathbf{F}_g + \mathbf{F}_s$, where the gradient force $\mathbf{F}_g$ is the conservative component, and the scattering force $\mathbf{F}_s$ is the nonconservative component. Both $\mathbf{F}_g$ and $\mathbf{F}_s$ originate from the scattering, but they play rather different roles in optical manipulation. The gradient force satisfies $\nabla \times \mathbf{F}_g = 0$, and the work done by $\mathbf{F}_g$ is always path independent. In consequence, one defines the optical potential energy ϕ to describe the gradient force $\mathbf{F}_g = -\nabla\phi$ and the negative sign indicates that the gradient force points in the direction of decreasing potential energy ϕ. The scattering force, on the other hand, satisfies $\nabla \cdot \mathbf{F}_s = 0$, and the work done by $\mathbf{F}_s$ is path dependent. Based on the optical Earnshaw theorem [7], it is impossible for $\mathbf{F}_s$ alone to construct any trap which needs to satisfy the necessary condition of stable equilibrium $\nabla \cdot \mathbf{F}_s < 0$ [9,10]. One defines the vector potential $\boldsymbol{\psi}$ to describe the scattering force $\mathbf{F}_s = \nabla \times \boldsymbol{\psi}$, and $\mathbf{F}_s$ is also termed the curl force [11].

One of the most important applications in optical micromanipulation is single-beam gradient force optical traps, which are usually described as optical tweezers [2–4,8]. The gradient force should be large enough for the dominating contributions in a stable optical trap. So previous researchers have tried to enhance the gradient force $\mathbf{F}_g$ and reduce the scattering force $\mathbf{F}_s$ by using a strongly focused beam from a high-numerical-aperture objective in experiments [2]. Unfortunately, the basic mechanism of splitting the optical force into the gradient force and scattering force for the spherical particle is only studied in the small-particle limit [7,12] and large-particle limit [8,13]. In the former (the particle's size parameter $x = kr \ll 1$, where k is the wave number in the background medium and r is the radius of the sphere), one can regard the particle as a dipole and obtain the gradient force and scattering force from the nonrelativistic Lorentz force by using Maxwell's equations [7,12]. In the large-particle limit ($x \gg 1$), an incident beam can be divided into a series of individual rays. Based on ray optics methods, the total force of each ray is further decomposed into the gradient and scattering forces, which are perpendicular and along the propagation direction of each ray,

*15110190043@fudan.edu.cn
†phlin@fudan.edu.cn

respectively [8]. Such approximate models are suitable only for either extremely small or large particles and cannot be used to separate the force for Mie particles, which are actually most accessible cases in the optical manipulation.

The generalized Lorenz-Mie theory (GLMT) [14–16], which is in terms of spherical harmonic expansions, can be used to deal with mechanical effects of light. GLMT bridges the gap between the dipole and the ray optics regimes, to which the theoretical part of the work by Ashkin was limited. However, the dependence of the optical force on the field quantities is totally masked in GLMT, and GLMT cannot decompose the gradient and scattering parts from the total force. So theoretically decomposing works of gradient force and scattering force are still confined to the approximation model in the dipole or ray optics regimes. In consequence, a standard setup of splitting the optical force suitable for particles of any size is essential for intensive study. Recently, Du and coworkers numerically split the optical force into gradient and scattering components via the Mie theory and fast Fourier transform [17]. However, their algorithm, falling into the category of nonlocal decomposition, needs to perform a great deal of calculation of the optical force over the whole physical space missing analytical expressions for either of these two force components for a more in-depth physical insight. More recently, Zheng and coworkers [18] presented an algorithm and computer codes for evaluating the gradient and scattering force components. Although ideally suited for the GLMT, their approach does not allow for deriving analytical expressions that show explicit dependence of the two force components on the illuminating optical fields, even in a simple optical field made up of a few interferential plane waves.

In this paper, we propose an alternative theoretical approach to split the optical force into gradient and scattering components. Following the previous work of Cartesian multipole expansion of the optical force [19,20] for general optical fields, we present a detailed process of decomposition through modeling the general monochromatic optical fields by a series of homogeneous plane waves, which has been justified by the expansion of the general monochromatic optical fields in terms of the regular vector spherical wave functions (VSWFs) as well as the integral representation of regular VSWFs (see [19]) for a rigorous proof. Our current approach belongs to the category of local decomposition, without having to resort to extensive computation of a massive number of data on optical force. Analytical expressions are derived for both conservative and nonconservative force components. As examples of application, we investigate the gradient force and scattering force acting on a dielectric particle of an arbitrary size immersed in Bessel beam and interferential multiple plane waves.

II. PROCESS OF DECOMPOSITION

In this section, we present a local decomposition of the time-averaged optical force $\langle \mathbf{F} \rangle$ acting on a sphere immersed in an arbitrary superposition of homogeneous plane waves based on the Cartesian multipole expansion theory, which is reviewed in Appendix A. It has been shown (see, e.g., [19,21]) that generic monochromatic optical fields can be written as a superposition of homogeneous plane waves. So our approach could be used to decompose $\langle \mathbf{F} \rangle$ acting on a sphere immersed in an arbitrary monochromatic optical field. Throughout the paper, we maintain a lossless background media with the wave vector $\mathbf{k}_i^2 = \omega^2/c^2$. Therefore the electric field $\mathbf{E}$ and magnetic field $\mathbf{B}$ consisting of n_p plane waves are expressed as

$$\mathbf{E} = \sum_{i=1}^{n_p} \mathbf{E}_i = \sum_{i=1}^{n_p} \mathcal{E}_i \, e^{i\mathbf{k}_i \cdot \mathbf{r}}, \quad \mathbf{B} = \sum_{i=1}^{n_p} \mathbf{B}_i = \sum_{i=1}^{n_p} \mathcal{B}_i \, e^{i\mathbf{k}_i \cdot \mathbf{r}}, \tag{1}$$

where spatial constant vectors $\mathcal{E}_i$ and $\mathcal{B}_i$ are the complex amplitudes of homogeneous plane waves, and satisfy

$$\mathbf{k}_i \cdot \mathcal{E}_i = 0, \quad \mathcal{B}_i = \frac{1}{\omega} \mathbf{k}_i \times \mathcal{E}_i. \tag{2}$$

Substituting Eqs. (1) into Eqs. (A1), the field moments of total optical fields can be expressed by the summation of each pair of plane waves, which is defined by subscripts i and j,

$$\mathbf{X}^{(n)} = \sum_{i,\,j} \mathbf{X}_{ij}^{(n)} = \sum_{i,\,j} x_{ij}^{n-1} \mathbf{X}_{ij}^{(1)}; \tag{3}$$

both i and j run from 1 to n_p. The field moments of each pair of plane waves are delineated by

$$\begin{aligned}
&D_{\mathrm{ee},\,ij}^{(n)} = x_{ij}^{n-1} D_{\mathrm{ee},\,ij}^{(1)}, \quad D_{\mathrm{mm},\,ij}^{(n)} = x_{ij}^{n-1} D_{\mathrm{mm},\,ij}^{(1)}, \\
&\mathbf{G}_{\mathrm{ee},\,ij}^{(n)} = x_{ij}^{n-1} \mathbf{G}_{\mathrm{ee},\,ij}^{(1)}, \\
&\mathbf{G}_{\mathrm{mm},\,ij}^{(n)} = x_{ij}^{n-1} \mathbf{G}_{\mathrm{mm},\,ij}^{(1)}, \quad \mathbf{G}_{\mathrm{em},\,ij}^{(n)} = x_{ij}^{n-1} \mathbf{G}_{\mathrm{em},\,ij}^{(1)}, \\
&\mathbf{G}_{\mathrm{me},\,ij}^{(n)} = x_{ij}^{n-1} \mathbf{G}_{\mathrm{me},\,ij}^{(1)}, \\
&\mathbf{S}_{\mathrm{ee},\,ij}^{(n)} = x_{ij}^{n-1} \mathbf{S}_{\mathrm{ee},\,ij}^{(1)}, \quad \mathbf{S}_{\mathrm{mm},\,ij}^{(n)} = x_{ij}^{n-1} \mathbf{S}_{\mathrm{mm},\,ij}^{(1)}, \\
&\mathbf{S}_{\mathrm{em},\,ij}^{(n)} = x_{ij}^{n-1} \mathbf{S}_{\mathrm{em},\,ij}^{(1)},
\end{aligned} \tag{4}$$

where $x_{ij} = (\mathbf{k}_i \cdot \mathbf{k}_j)$, and

$$\begin{aligned}
D_{\mathrm{ee},\,ij}^{(1)} &= (\mathcal{E}_i \cdot \mathcal{E}_j^*) \, e^{i(\mathbf{k}_i - \mathbf{k}_j)\cdot \mathbf{r}}, \\
D_{\mathrm{mm},\,ij}^{(1)} &= (\mathcal{B}_i \cdot \mathcal{B}_j^*) \, e^{i(\mathbf{k}_i - \mathbf{k}_j)\cdot \mathbf{r}}, \\
\mathbf{G}_{\mathrm{ee},\,ij}^{(1)} &= -i(\mathbf{k}_j \cdot \mathcal{E}_i) \, \mathcal{E}_j^* \, e^{i(\mathbf{k}_i - \mathbf{k}_j)\cdot \mathbf{r}}, \\
\mathbf{G}_{\mathrm{mm},\,ij}^{(1)} &= -i(\mathbf{k}_j \cdot \mathcal{B}_i) \, \mathcal{B}_j^* \, e^{i(\mathbf{k}_i - \mathbf{k}_j)\cdot \mathbf{r}}, \\
\mathbf{G}_{\mathrm{em},\,ij}^{(1)} &= -i(\mathbf{k}_j \cdot \mathcal{E}_i) \, \mathcal{B}_j^* \, e^{i(\mathbf{k}_i - \mathbf{k}_j)\cdot \mathbf{r}}, \\
\mathbf{G}_{\mathrm{me},\,ij}^{(1)} &= -i(\mathbf{k}_j \cdot \mathcal{B}_i) \, \mathcal{E}_j^* \, e^{i(\mathbf{k}_i - \mathbf{k}_j)\cdot \mathbf{r}}, \\
\mathbf{S}_{\mathrm{ee},\,ij}^{(1)} &= (\mathcal{E}_i \times \mathcal{E}_j^*) \, e^{i(\mathbf{k}_i - \mathbf{k}_j)\cdot \mathbf{r}}, \\
\mathbf{S}_{\mathrm{mm},\,ij}^{(1)} &= (\mathcal{B}_i \times \mathcal{B}_j^*) \, e^{i(\mathbf{k}_i - \mathbf{k}_j)\cdot \mathbf{r}}, \\
\mathbf{S}_{\mathrm{em},\,ij}^{(1)} &= (\mathcal{E}_i \times \mathcal{B}_j^*) \, e^{i(\mathbf{k}_i - \mathbf{k}_j)\cdot \mathbf{r}}.
\end{aligned} \tag{5}$$

In the case of homogeneous plane waves, all terms turn to constants when $i = j$ in Eqs. (4) and (5). Inserting Eqs. (4) and (5) into Eqs. (A5), $\mathbf{Z}_{\mathrm{ee},ij}^{(n)}$ and $\mathbf{Z}_{\mathrm{mm},ij}^{(n)}$ for each pair of plane waves are represented by $\mathbf{Z}_{\mathrm{ee},ij}^{(1)}$ and $\mathbf{Z}_{\mathrm{mm},ij}^{(1)}$,

$$\mathbf{Z}_{\mathrm{ee}}^{(n)} = \sum_{i,\,j} x_{ij}^{n-1} \mathbf{Z}_{\mathrm{ee},ij}^{(1)}, \quad \mathbf{Z}_{\mathrm{mm}}^{(n)} = \sum_{i,\,j} x_{ij}^{n-1} \mathbf{Z}_{\mathrm{mm},ij}^{(1)}, \tag{6}$$

where

$$\mathbf{Z}^{(1)}_{\mathrm{ee},ij} = \frac{1}{2}\big[\nabla D^{(1)}_{\mathrm{ee},ij} - \nabla\times\mathbf{S}^{(1)}_{\mathrm{ee},ij} - 2i\omega\,\mathrm{Re}\,\mathbf{S}^{(1)}_{\mathrm{em},ij}\big],$$
$$\mathbf{Z}^{(1)}_{\mathrm{mm},ij} = \frac{1}{2}\left[\nabla D^{(1)}_{\mathrm{mm},ij} - \nabla\times\mathbf{S}^{(1)}_{\mathrm{mm},ij} - \frac{2i\omega}{c^2}\,\mathrm{Re}\,\mathbf{S}^{(1)}_{\mathrm{em},ij}\right]. \quad (7)$$

In the case of a single wave vector (namely, $i = j$ here), $\mathbf{S}^{(1)}_{\mathrm{em},\,ij}$ is solenoidal in our treatment [22],

$$\mathbf{S}^{(1)\mathrm{grad}}_{\mathrm{em},\,ii} = 0, \quad \mathbf{S}^{(1)\mathrm{curl}}_{\mathrm{em},\,ii} = \mathcal{E}_i\times\mathcal{B}^*_i, \quad (8)$$

where summations of $\mathbf{S}^{(1)\mathrm{curl}}_{\mathrm{em},\,ii}$ correspond to the constant real vector $\mathbf{P}^{(n)}$ in Eq. (A19). In the case of $i \neq j$, substituting Eqs. (4) and (5) into Eqs. (A18) and using the series expansion of $1/(1-x)$, $\mathbf{S}^{(n)}_{\mathrm{em},ij}$ is decomposed as follows:

$$\mathbf{S}^{(1)\mathrm{grad}}_{\mathrm{em},\,ij} = -\frac{i}{2(1-x_{ij})}\nabla\big[D^{(1)}_{\mathrm{mm},ij} - D^{(1)}_{\mathrm{ee},ij}\big],$$
$$\mathbf{S}^{(1)\mathrm{curl}}_{\mathrm{em},\,ij} = -\frac{1}{2(1-x_{ij})}\nabla\times\big[\mathbf{G}^{(1)}_{\mathrm{em},ij} - \mathbf{G}^{(1)*}_{\mathrm{me},ji}\big]. \quad (9)$$

Meanwhile $\mathbf{Z}^{(1)}_{\mathrm{ee},ij}$ and $\mathbf{Z}^{(1)}_{\mathrm{mm},ij}$ are decomposed:

$$\mathbf{Z}^{(1)\mathrm{gr}}_{\mathrm{ee},\,ij} = \tfrac{1}{2}\nabla D^{(1)}_{\mathrm{ee},\,ij},$$
$$\mathbf{Z}^{(1)\mathrm{cr}}_{\mathrm{ee},\,ij} = -\tfrac{1}{2}\nabla\times\mathbf{S}^{(1)}_{\mathrm{ee},\,ij} - i\,\mathrm{Re}\,\mathbf{S}^{(1)}_{\mathrm{em},\,ij},$$
$$\mathbf{Z}^{(1)\mathrm{gr}}_{\mathrm{mm},\,ij} = \tfrac{1}{2}\nabla D^{(1)}_{\mathrm{mm},\,ij},$$
$$\mathbf{Z}^{(1)\mathrm{cr}}_{\mathrm{mm},\,ij} = -\tfrac{1}{2}\nabla\times\mathbf{S}^{(1)}_{\mathrm{mm},\,ij} - i\,\mathrm{Re}\,\mathbf{S}^{(1)}_{\mathrm{em},\,ij}. \quad (10)$$

One can note that $\mathrm{Re}\,\mathbf{S}^{(1)}_{\mathrm{em},\,ij}$ is no longer purely solenoidal due to the complex moments $D^{(1)}_{\mathrm{ee},\,ij}$ and $D^{(1)}_{\mathrm{mm},\,ij}$ in Eqs. (9). As a consequence, the superscripts "gr" and "cr" of $\mathbf{Z}^{(1)}_{\mathrm{ee},\,ij}$ and $\mathbf{Z}^{(1)}_{\mathrm{mm},\,ij}$ in Eqs. (10) correspond to the gradient force and scattering force, whereas they are not the irrotational and solenoidal components. In the following, we analytically prove that the irrotational part of $\mathrm{Re}\,\mathbf{S}^{(1)}_{\mathrm{em},\,ij}$ makes no contribution to the gradient forces. Using the identity for homogeneous plane waves

$$t_{ij} = (\mathbf{k}_i - \mathbf{k}_j)\cdot(\mathcal{E}_i\times\mathcal{B}^*_j) \equiv \mathcal{B}_i\cdot\mathcal{B}^*_j - \mathcal{E}_i\cdot\mathcal{E}^*_j, \quad (11)$$

we obtain that t_{ji} is the complex conjugate of t_{ij}. Then it is clearly seen from Eqs. (4) that

$$\nabla\cdot\mathbf{S}^{(1)}_{\mathrm{em},\,ij} = i(\mathbf{k}_i - \mathbf{k}_j)\cdot(\mathcal{E}_i\times\mathcal{B}^*_j)\,e^{i(\mathbf{k}_i-\mathbf{k}_j)\cdot\mathbf{r}}$$
$$= i\,t_{ij}\,e^{i(\mathbf{k}_i-\mathbf{k}_j)\cdot\mathbf{r}} \quad (12)$$

is the complex conjugate of $[-\nabla\cdot\mathbf{S}^{(1)}_{\mathrm{em},\,ji}]$, so that the identity

$$\nabla\cdot\mathrm{Re}\big[\mathbf{S}^{(1)}_{\mathrm{em},\,ij}\big] + \nabla\cdot\mathrm{Re}\big[\mathbf{S}^{(1)}_{\mathrm{em},\,ji}\big] \equiv 0 \quad (13)$$

is established for each pair of plane waves. As a consequence, although $\mathrm{Re}\,\mathbf{S}^{(1)}_{\mathrm{em},\,ij}$ has irrotational parts along with $\nabla\cdot\mathrm{Re}\,\mathbf{S}^{(1)}_{\mathrm{em},\,ij} \neq 0$, the summation of $\mathrm{Re}\,\mathbf{S}^{(1)}_{\mathrm{em},\,ij}$ over all pairs of homogenous plane waves is purely solenoidal with $\nabla\cdot\sum_{i,\,j}\mathrm{Re}\,\mathbf{S}^{(1)}_{\mathrm{em},\,ij} = 0$. Meanwhile, both $\nabla\cdot\mathbf{Z}^{(1)\mathrm{cr}}_{\mathrm{ee},\,ij} \neq 0$ and $\nabla\cdot\mathbf{Z}^{(1)\mathrm{cr}}_{\mathrm{mm},\,ij} \neq 0$ in Eqs. (10), but summing over all pairs of plane waves satisfies $\nabla\cdot\sum_{i,\,j}\mathbf{Z}^{(1)\mathrm{cr}}_{\mathrm{ee},\,ij} = 0$ and $\nabla\cdot\sum_{i,\,j}\mathbf{Z}^{(1)\mathrm{cr}}_{\mathrm{mm},\,ij} = 0$. Considering that each pair of plane waves satisfies $x_{ij} = x_{ji}$ and shares the same coefficients $Q^{(n)}_{l,\,ij} = Q^{(n)}_{l,\,ji}$ or $R^{(n)}_{l,\,ij} = R^{(n)}_{l,\,ji}$, then $\mathbf{Z}^{(1)\mathrm{cr}}_{\mathrm{ee},\,ij}$ and $\mathbf{Z}^{(1)\mathrm{cr}}_{\mathrm{mm},\,ij}$ contribute only to the scattering forces. In the case of a single plane wave, $\mathbf{Z}^{(1)}_{\mathrm{ee},ii}$ and $\mathbf{Z}^{(1)}_{\mathrm{mm},ii}$ are attributed to the scattering force because both $D^{(1)}_{\mathrm{ee},\,ii}$ and $D^{(1)}_{\mathrm{mm},\,ii}$ are independent of $\mathbf{r}$ in Eqs. (5), which lead to $\nabla D^{(1)}_{\mathrm{ee},\,ii} = \nabla D^{(1)}_{\mathrm{mm},\,ii} = 0$ in Eqs. (10). As a consequence, the total force of a single plane wave is completely attributed to the scattering force.

The total optical force, which is the full Lorentz-Maxwell force exerted on the particle, can be divided into the extinction (interception) force and recoil force. The electric (magnetic) part of extinction forces, i.e., $\langle\mathbf{F}^{\mathrm{e}(l)}_{\mathrm{int}}\rangle$ ($\langle\mathbf{F}^{\mathrm{m}(l)}_{\mathrm{int}}\rangle$), is generated by the interaction between the electric (magnetic) multipoles and the external electric (magnetic) field. The corresponding electric (magnetic) polarizability $\gamma^{(l)}_{\mathrm{elec}}$ ($\gamma^{(l)}_{\mathrm{mag}}$) in Appendix A is proportional to the Mie coefficient a_l (b_l) in the GLMT [14–16]. On the other hand, the recoil forces are generated by the coupling between the electric multipoles of adjacent orders (electric part, i.e., $\langle\mathbf{F}^{\mathrm{e}(l)}_{\mathrm{rec}}\rangle$), magnetic multipoles of adjacent orders (magnetic part, i.e., $\langle\mathbf{F}^{\mathrm{m}(l)}_{\mathrm{rec}}\rangle$), and electric and magnetic multipoles of the same order (hybrid part, i.e., $\langle\mathbf{F}^{\mathrm{x}(l)}_{\mathrm{rec}}\rangle$). One can note that the existence of recoil forces violates Newton's third law in electrodynamics.

In Appendix B, we give the extinction and recoil forces of arbitrary superposition of homogeneous plane waves in terms of Legendre polynomials, which can avoid numerical instability for large orders. Every component in Eqs. (B11) and (B12) consists of $\mathbf{Z}^{(1)}_{\mathrm{ee},ij}$, $\mathbf{Z}^{(1)}_{\mathrm{mm},ij}$, $\mathbf{S}^{(1)}_{\mathrm{em},ij}$, and their complex conjugates, which are decomposed in Eqs. (9) and (10). Finally, the extinction and recoil forces in Eqs. (B11) and (B12) are decomposed into the gradient force and scattering force as

$$\big\langle\mathbf{F}^{\mathrm{e}(l)}_{\mathrm{int}}\big\rangle_{\mathrm{grad}} = u^{(1)}_l\mathrm{Im}\sum_{i,\,j}a_l\big[Q^{(1)}_{l,\,ij}\mathbf{Z}^{(1)\mathrm{gr}}_{\mathrm{ee},\,ij} - Q^{(2)}_{l,\,ij}\mathbf{Z}^{(1)\mathrm{gr}}_{\mathrm{mm},\,ij}\big], \quad (14a)$$

$$\big\langle\mathbf{F}^{\mathrm{e}(l)}_{\mathrm{int}}\big\rangle_{\mathrm{curl}} = u^{(1)}_l\mathrm{Im}\sum_{i,\,j}a_l\big[Q^{(1)}_{l,\,ij}\mathbf{Z}^{(1)\mathrm{cr}}_{\mathrm{ee},\,ij} - Q^{(2)}_{l,\,ij}\mathbf{Z}^{(1)\mathrm{cr}}_{\mathrm{mm},\,ij}\big], \quad (14b)$$

$$\big\langle\mathbf{F}^{\mathrm{m}(l)}_{\mathrm{int}}\big\rangle_{\mathrm{grad}} = u^{(1)}_l\mathrm{Im}\sum_{i,\,j}b_l\big[Q^{(1)}_{l,\,ij}\mathbf{Z}^{(1)\mathrm{gr}}_{\mathrm{mm},\,ij} - Q^{(2)}_{l,\,ij}\mathbf{Z}^{(1)\mathrm{gr}}_{\mathrm{ee},\,ij}\big], \quad (14c)$$

$$\big\langle\mathbf{F}^{\mathrm{m}(l)}_{\mathrm{int}}\big\rangle_{\mathrm{curl}} = u^{(1)}_l\mathrm{Im}\sum_{i,\,j}b_l\big[Q^{(1)}_{l,\,ij}\mathbf{Z}^{(1)\mathrm{cr}}_{\mathrm{mm},\,ij} - Q^{(2)}_{l,\,ij}\mathbf{Z}^{(1)\mathrm{cr}}_{\mathrm{ee},\,ij}\big], \quad (14d)$$

and

$$\left\langle \mathbf{F}_{\mathrm{rec}}^{\mathrm{e}(l)} \right\rangle_{\mathrm{grad}} = u_l^{(2)} \mathrm{Im} \sum_{i,j} a_{l+1} a_l^* \left[R_{l,ij}^{(1)} \left(\mathbf{Z}_{\mathrm{ee},ij}^{(1)\mathrm{gr}} \right)^* - R_{l,ij}^{(2)} \left(\mathbf{Z}_{\mathrm{mm},ij}^{(1)\mathrm{gr}} \right)^* - 4iR_{l,ij}^{(3)} \left(\mathbf{S}_{\mathrm{em},ij}^{(1)\mathrm{grad}} \right)^* \right.$$
$$\left. + R_{l,ij}^{(4)} \mathbf{Z}_{\mathrm{ee},ij}^{(1)\mathrm{gr}} - R_{l,ij}^{(5)} \mathbf{Z}_{\mathrm{mm},ij}^{(1)\mathrm{gr}} + 4iR_{l,ij}^{(6)} \mathbf{S}_{\mathrm{em},ij}^{(1)\mathrm{grad}} \right], \tag{15a}$$

$$\left\langle \mathbf{F}_{\mathrm{rec}}^{\mathrm{e}(l)} \right\rangle_{\mathrm{curl}} = u_l^{(2)} \mathrm{Im} \sum_{i,j} a_{l+1} a_l^* \left[R_{l,ij}^{(1)} \left(\mathbf{Z}_{\mathrm{ee},ij}^{(1)\mathrm{cr}} \right)^* - R_{l,ij}^{(2)} \left(\mathbf{Z}_{\mathrm{mm},ij}^{(1)\mathrm{cr}} \right)^* - 4iR_{l,ij}^{(3)} \left(\mathbf{S}_{\mathrm{em},ij}^{(1)\mathrm{curl}} \right)^* \right.$$
$$\left. + R_{l,ij}^{(4)} \mathbf{Z}_{\mathrm{ee},ij}^{(1)\mathrm{cr}} - R_{l,ij}^{(5)} \mathbf{Z}_{\mathrm{mm},ij}^{(1)\mathrm{cr}} + 4iR_{l,ij}^{(6)} \mathbf{S}_{\mathrm{em},ij}^{(1)\mathrm{curl}} \right], \tag{15b}$$

$$\left\langle \mathbf{F}_{\mathrm{rec}}^{\mathrm{m}(l)} \right\rangle_{\mathrm{grad}} = u_l^{(2)} \mathrm{Im} \sum_{i,j} b_{l+1} b_l^* \left[R_{l,ij}^{(1)} \left(\mathbf{Z}_{\mathrm{mm},ij}^{(1)\mathrm{gr}} \right)^* - R_{l,ij}^{(2)} \left(\mathbf{Z}_{\mathrm{ee},ij}^{(1)\mathrm{gr}} \right)^* - 4iR_{l,ij}^{(3)} \mathbf{S}_{\mathrm{em},ij}^{(1)\mathrm{grad}} \right.$$
$$\left. + R_{l,ij}^{(4)} \mathbf{Z}_{\mathrm{mm},ij}^{(1)\mathrm{gr}} - R_{l,ij}^{(5)} \mathbf{Z}_{\mathrm{ee},ij}^{(1)\mathrm{gr}} + 4iR_{l,ij}^{(6)} \left(\mathbf{S}_{\mathrm{em},ij}^{(1)\mathrm{grad}} \right)^* \right], \tag{15c}$$

$$\left\langle \mathbf{F}_{\mathrm{rec}}^{\mathrm{m}(l)} \right\rangle_{\mathrm{curl}} = u_l^{(2)} \mathrm{Im} \sum_{i,j} b_{l+1} b_l^* \left[R_{l,ij}^{(1)} \left(\mathbf{Z}_{\mathrm{mm},ij}^{(1)\mathrm{cr}} \right)^* - R_{l,ij}^{(2)} \left(\mathbf{Z}_{\mathrm{ee},ij}^{(1)\mathrm{cr}} \right)^* - 4iR_{l,ij}^{(3)} \mathbf{S}_{\mathrm{em},ij}^{(1)\mathrm{curl}} \right.$$
$$\left. + R_{l,ij}^{(4)} \mathbf{Z}_{\mathrm{mm},ij}^{(1)\mathrm{cr}} - R_{l,ij}^{(5)} \mathbf{Z}_{\mathrm{ee},ij}^{(1)\mathrm{cr}} + 4iR_{l,ij}^{(6)} \left(\mathbf{S}_{\mathrm{em},ij}^{(1)\mathrm{curl}} \right)^* \right], \tag{15d}$$

$$\left\langle \mathbf{F}_{\mathrm{rec}}^{\mathrm{x}(l)} \right\rangle_{\mathrm{grad}} = u_l^{(3)} \mathrm{Im} \sum_{i,j} a_l b_l^* \left\{ R_{l,ij}^{(4)} \left[\mathbf{Z}_{\mathrm{mm},ij}^{(1)\mathrm{gr}} - \left(\mathbf{Z}_{\mathrm{ee},ij}^{(1)\mathrm{gr}} \right)^* \right] + 4iR_{l,ij}^{(6)} \left(\mathbf{S}_{\mathrm{em},ij}^{(1)\mathrm{grad}} \right)^* \right.$$
$$\left. + R_{l,ij}^{(5)} \left[\left(\mathbf{Z}_{\mathrm{mm},ij}^{(1)\mathrm{gr}} \right)^* - \mathbf{Z}_{\mathrm{ee},ij}^{(1)\mathrm{gr}} \right] + 4iR_{l,ij}^{(7)} \mathbf{S}_{\mathrm{em},ij}^{(1)\mathrm{grad}} \right\}, \tag{15e}$$

$$\left\langle \mathbf{F}_{\mathrm{rec}}^{\mathrm{x}(l)} \right\rangle_{\mathrm{curl}} = u_l^{(3)} \mathrm{Im} \sum_{i,j} a_l b_l^* \left\{ R_{l,ij}^{(4)} \left[\mathbf{Z}_{\mathrm{mm},ij}^{(1)\mathrm{cr}} - \left(\mathbf{Z}_{\mathrm{ee},ij}^{(1)\mathrm{cr}} \right)^* \right] + 4iR_{l,ij}^{(6)} \left(\mathbf{S}_{\mathrm{em},ij}^{(1)\mathrm{curl}} \right)^* \right.$$
$$\left. + R_{l,ij}^{(5)} \left[\left(\mathbf{Z}_{\mathrm{mm},ij}^{(1)\mathrm{cr}} \right)^* - \mathbf{Z}_{\mathrm{ee},ij}^{(1)\mathrm{cr}} \right] + 4iR_{l,ij}^{(7)} \mathbf{S}_{\mathrm{em},ij}^{(1)\mathrm{curl}} \right\}, \tag{15f}$$

where the Mie coefficients are a_l and b_l [23], with

$$Q_{l,ij}^{(1)} = \sum_{m=1}^{l} {}^{(2)} m(2l+1-m)(2l+1-2m) P_{l-m}(x_{ij}), \tag{16a}$$

$$Q_{l,ij}^{(2)} = \sum_{m=2}^{l} {}^{(2)} m(2l+1-m)(2l+1-2m) P_{l-m}(x_{ij}), \tag{16b}$$

$$R_{l,ij}^{(1)} = \sum_{m=1}^{l} {}^{(2)} (m+1)(2l+2-m)(2l+1-2m)[2(m+1)l - (m^2-m-4)] P_{l-m}(x_{ij}), \tag{16c}$$

$$R_{l,ij}^{(2)} = \sum_{m=2}^{l} {}^{(2)} m(m+2)(2l+1-m)(2l+1-2m)(2l+3-m) P_{l-m}(x_{ij}), \tag{16d}$$

$$R_{l,ij}^{(3)} = \sum_{m=1}^{l} {}^{(2)} (m+1)(2l+2-m)(2l+1-2m) P_{l-m}(x_{ij}), \tag{16e}$$

$$R_{l,ij}^{(4)} = \sum_{m=2}^{l} {}^{(2)} (2l+1-m)(2l+1-2m)[2m^2 l - m(m+1)(m-2)] P_{l-m}(x_{ij}), \tag{16f}$$

$$R_{l,ij}^{(5)} = \sum_{m=1}^{l} {}^{(2)} (m+1)(m-1)(2l-m)(2l+2-m)(2l+1-2m) P_{l-m}(x_{ij}), \tag{16g}$$

$$R_{l,ij}^{(6)} = \sum_{m=2}^{l} {}^{(2)} m(2l+1-m)(2l+1-2m) P_{l-m}(x_{ij}), \tag{16h}$$

$$R_{l,ij}^{(7)} = \sum_{m=1}^{l} {}^{(2)} (2l+1-2m)[2l^2 - 2(m-1)l + m^2 - m] P_{l-m}(x_{ij}). \tag{16i}$$

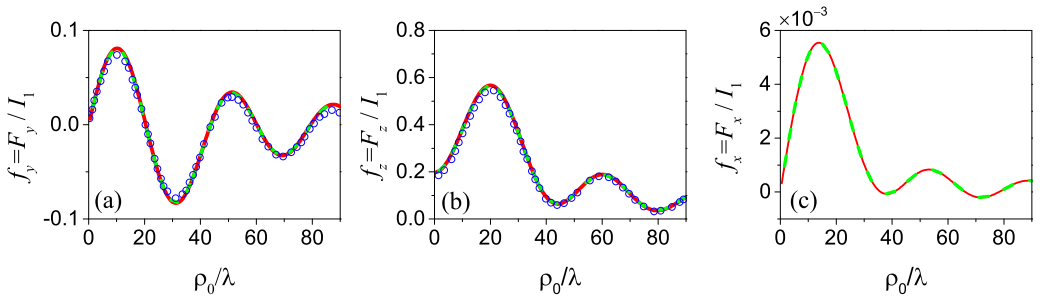

FIG. 1. Normalized optical force components f_y, f_z, and f_x exerted on a dielectric sphere (radius $r_0 = 10\lambda$, refractive index $n_s = 2$) in the circular polarized Bessel beam versus the displacement of the beam center ρ_0 along the $+y$ direction. (a) Force component f_y as a function of displacement ρ_0. Solid red curves and dashed green curves are based on the multipole decomposition method and Mie theory, respectively, while blue circles are based on the ray optics method from Ref. [30]. (b, c) Same as (a) except for the force components f_z and f_x.

The summation indices of $\sum_{m=1}^{l}{}^{(2)}$ and $\sum_{m=2}^{l}{}^{(2)}$ denote the index m odd and even positive integers satisfying $0 < m \leqslant n$, and $P_m(x)$ is the Legendre polynomial. Equations (14) and (15) represent the fundamental formulation for the decomposition of optical force into the conservative (gradient) and nonconservative (scattering) components. The final expressions were summarized in Ref. [24] and we present the comprehensive derivation in this paper.

III. NUMERICAL RESULTS AND DISCUSSION

With formulations given in the previous section, we calculate the gradient and scattering forces acting on a dielectric particle immersed in Bessel beams and interferential multiple plane waves, respectively. The comparison with the ray optics method of Bessel beams is also exhibited.

A. Bessel beams

In this section, we divide a Bessel beam into a series of plane waves via the angular spectrum representation [21]. Then the gradient force and scattering force can be calculated for a spherical particle illuminated by the Bessel beam. The angular spectrum of the Bessel beam is described by plane waves with wave vectors lying on the conical surface with fixed polar angle α_0, which means the angular spectrum representation can be formulated in terms of one-dimensional integration over the azimuthal angle β. Therefore the angular spectrum of the electric field is defined in Cartesian coordinates [25–27],

$$\mathbf{E}_{\mathrm{B}}(r,\theta,\phi) = -\frac{1}{2\pi} i^l e^{ikr\cos\alpha_0\cos\theta} \times \int_{\beta=0}^{2\pi} e^{il\beta} e^{ikr\sin\alpha_0\sin\theta\cos(\phi-\beta)} \mathbf{Q} d\beta, \quad (17)$$

with

$$\mathbf{Q} = (c_2\cos\alpha_0\cos\beta + c_1\sin\beta)\mathbf{e}_x + (c_2\cos\alpha_0\sin\beta - c_1\cos\beta)\mathbf{e}_y - c_2\sin\alpha_0\mathbf{e}_z. \quad (18)$$

The integrations in Eq. (17) are already worked out, and the explicit expressions in cylindrical coordinates are listed below [25–27],

$$\mathbf{E}_{\mathrm{B}}(r,\theta,\phi) = ic_1\mathbf{M}_l^{(c)}(\rho,\phi,z) + c_2\mathbf{N}_l^{(c)}(\rho,\phi,z), \quad (19)$$

where vector cylindrical wave functions are defined by [25]

$$\mathbf{M}_l^{(c)}(\rho,\phi,z) = \left[\frac{il}{a\rho}J_l(a\rho)\mathbf{e}_r - J_l'(a\rho)\mathbf{e}_\phi\right]e^{il\phi+ibz},$$
$$\mathbf{N}_l^{(c)}(\rho,\phi,z) = \frac{a}{k}J_l(a\rho)e^{il\phi+ibz}\mathbf{e}_z + \frac{ib}{k}\mathbf{e}_z\times\mathbf{M}_l^{(c)}, \quad (20)$$

with $\rho = r\sin\theta$, $z = r\cos\theta$, $a = k\sin\alpha_0$, and $b = k\cos\alpha_0$ [27]. We use the Gauss quadrature formulas [28,29] to rewrite Eq. (17) as a summation, for which each group of the Gaussian abscissas β_i and weights w_i corresponds to a homogeneous plane wave with the electric field components in Cartesian coordinates,

$$E_x^i = -\frac{w_i}{2\pi}i^l(c_2\cos\alpha_0\cos\beta_i + c_1\sin\beta_i),$$
$$E_y^i = -\frac{w_i}{2\pi}i^l(c_2\cos\alpha_0\sin\beta_i - c_1\cos\beta_i),$$
$$E_z^i = \frac{w_i}{2\pi}i^l c_2\sin\alpha_0. \quad (21)$$

Consequently, each group of plane waves can be determined by α_0, β_i, p_1^i, and p_2^i, where p_1^i and p_2^i are the same as Eqs. (24):

$$p_1^i = -E_z^i/\sin\alpha_0, \quad p_2^i = \cos\beta_i E_y^i - \sin\beta_i E_x^i. \quad (22)$$

To corroborate the method, we calculate the optical force exerted on a sphere illuminated by a circular polarized Bessel beam. Parameters of the Bessel beam are the same as in Ref. [30], i.e., the order $l = 2$, coefficients $c_1 = -i$, $c_2 = k/b$, and cone angle $\alpha_0 = 0.0141$ in Eq. (17). Parameters of the dielectric sphere are fixed to radius $r_0 = 10\lambda$ and relative refractive index $n_s = 2$. Three force components, normalized by the intensity $I_1 = \varepsilon_0 E_0^2 r_0^2$, as a function of the beam center's displacement ρ_0 along the $+y$ direction are given in Fig. 1. The results based on our approach (red lines), obtained by 35 plane waves, confirm that the component f_y is gradient force, while the components f_z and f_x are scattering forces. Compared with the total force based on the Mie theory (dashed green curves), perfect agreement is reached in Fig. 1. Comparing our approach with the data of previous work based on the ray optics method (blue circles) [30], in which the force component f_x is ignored, a visible difference in the gradient force f_y and scattering force f_z is shown in Figs. 1(a) and 1(b). Definitions of the relative errors $\delta_g = (f_g^r - f_g^m)/f_g^r$ and $\delta_s =$

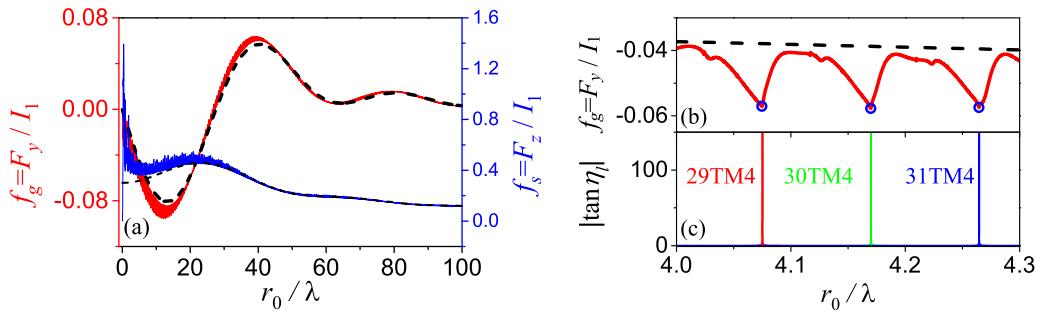

FIG. 2. (a) Normalized optical force components f_g and f_s versus the normalized radius r_0/λ. Gradient force f_g (left axis; red line) and scattering force f_s (right axis; blue line) based on the multipole expansion method; dashed black lines based on the ray optics method. (b) Enlarged view of (a) in the range of $4\lambda < r_0 < 4.3\lambda$. (c) Moduli of scattering phases $|\tan \eta_l|$ in the range $4\lambda < r_0 < 4.3\lambda$.

$(f_s^r - f_s^m)/f_s^r$ are given in Ref. [30], where the superscripts r and m denote results calculated by ray optics [30] and our multipole decomposition method, respectively. The relative error is $|\delta_g| \approx 8\%$ for $\rho_0 = 10\lambda$ in Fig. 1(a) and $|\delta_s| \approx 4\%$ for $\rho_0 = 20\lambda$ in Fig. 1(b). Considering the ray optics method suitable for spheres large enough, the relative error would become larger with decreasing radius.

The gradient force and scattering force versus the normalized radius r_0/λ are presented in Fig. 2. Considering that the scattering force component f_x is smaller than f_z by two orders of magnitude in Fig. 1, we set the normalized gradient force $f_g = F_y/I_1$ and the scattering force $f_s = F_z/I_1$ in Fig. 2. The displacement is fixed to $\rho_0 = 10\lambda$ and other parameters are the same as in Fig. 1. There is a large difference between our method (solid curves) and the ray optics method (dashed curves) for $r_0 < 5\lambda$. And it is evident that the results of the two methods are close to each other for $r_0 > 20\lambda$ in Fig. 2(a). Both the gradient force and the scattering force display oscillations by our method, however, such oscillations do not exist in the ray optics regime (dashed black curves). An enlarged view of the gradient force is shown in Fig. 2(b). We confirm that the gradient force displays oscillations (solid red curves) with three notable peaks (blues circles) by our method, while the curve is smooth by the ray optics method. In Fig. 2(c), the moduli of scattering phases of the sphere are exhibited in the same range as in Fig. 2(b). The transverse magnetic (TM) scattering phases, depending on the Mie coefficients b_l, are expressed as $\tan \eta_l = -ib_l/(b_l - 1)$ and labeled (l)TM(n), where l and n are the orders and modes [31–33]. Comparing Fig. 2(b) with Fig. 2(c), three force peaks are associated with three scattering phase peaks at $r_0 = 4.075\lambda$, $r_0 = 4.170\lambda$, and $r_0 = 4.265\lambda$ separately. As a consequence, oscillations in Fig. 2(a) correspond to Mie resonances.

B. Interferential multiple plane waves

In this section, we calculate the gradient force and scattering force acting on a spherical particle of arbitrary size immersed in interferential multiple plane waves. We concentrate on homogeneous plane waves with real polar angles α and azimuthal angles β of wave vectors $\mathbf{k}$, which is a special case of complex wave vector fields [34],

$$\begin{aligned}\mathbf{E}_{\text{inc}} &= \mathbf{E}\, e^{i\mathbf{k}\cdot\mathbf{r}} = E_0(E_x\mathbf{e}_x + E_y\mathbf{e}_y + E_z\mathbf{e}_z)e^{i(k_x r_x + k_y r_y + k_z r_z)} \\ &= E_0(p_1\,\boldsymbol{\theta}_k + p_2\,\boldsymbol{\phi}_k)e^{i(k_x r_x + k_y r_y + k_z r_z)}, \end{aligned} \tag{23}$$

where $\mathbf{e}_x$, $\mathbf{e}_y$, and $\mathbf{e}_z$ are the unit vectors in the Cartesian coordinate system, $\boldsymbol{\theta}_k$ and $\boldsymbol{\phi}_k$ are the unit vectors in the spherical coordinate system, and $E_0 > 0$ denotes the amplitude. p_1 and p_2 correspond to the complex amplitudes of p and s polarizations, and three Cartesian components of wave vector $\mathbf{k}$ can be expressed by α and β,

$$\begin{aligned} &p_1 = -E_z/\sin\alpha, \quad p_2 = \cos\beta E_y - \sin\beta E_x, \\ &k_x = k\sin\alpha\cos\beta, \quad k_y = k\sin\alpha\sin\beta, \quad k_z = k\cos\beta, \end{aligned} \tag{24}$$

where $k = 2\pi n_d/\lambda$, with λ denoting the wavelength in vacuum and relative refractive index n_d of the surrounding medium. The dielectric sphere ($n_s = \sqrt{3}$) is immersed in water ($n_d = 1.33$) and the center of the sphere is fixed to $(\lambda/3, 0, 0)$. The operating wavelength is fixed at $\lambda = 1064$ nm. Therefore a plane wave can be depicted by the parameters, i.e., α, β, p_1, and p_2, with α in the range$0 < \alpha < 180^\circ$ and β in the range $0 < \beta < 360^\circ$. We choose a group of parameters of 10 plane waves in Table I.

The optical force components f_x, f_y, and f_z, normalized by $I_2 = \varepsilon_0 E_0^2/k_0^2$, as a function of the spherical radius in the range $0 < r_0 < 50\lambda$ are shown in Fig. 3. Mie resonances of the dielectric sphere are also visible in Fig. 3, while they disappeared at a wide radius interval. Using our approach, the gradient components f_g (dashed red curves), the scattering components f_s (solid red curves), and their summations f_t (dashed green curves) acting on the particle by the 10 interferential plane waves are calculated. Using the Mie theory in previous work [34], the total force of 10 interferential plane

TABLE I. Data on 10 plane waves.

	α	β	p_1	p_2
pw_1	2°	122°	$1.0324 + 0.3441i$	1.0324
pw_2	3°	149°	$-0.5040 + 0.2520i$	$0.2520 + 0.2520i$
pw_3	4°	331°	$-0.1667 - 0.1667i$	$0.1667 - 0.1667i$
pw_4	5°	236°	$0.4364 - 0.6547i$	$-0.4364 + 0.4364i$
pw_5	6°	88°	$-0.9383 + 0.3128i$	$-0.6255 - 0.9383i$
pw_6	7°	218°	$0.2085 - 0.4170i$	$0.6255 + 0.6255i$
pw_7	7°	227°	$-0.4588 + 1.3765i$	$1.3765i$
pw_8	8°	353°	$-0.2395 - 0.3592i$	$0.3592 - 0.3592i$
pw_9	9°	332°	$-0.6708 + 0.2236i$	$0.6708 + 0.2236i$
pw_{10}	10°	138°	$0.3873 - 0.1291i$	$-0.2582 - 0.1291i$

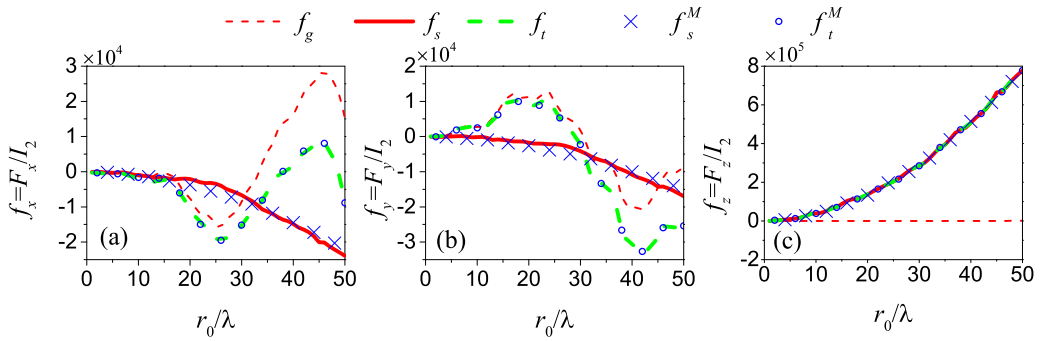

FIG. 3. Normalized optical force components f_x, f_y, and f_z acting on a dielectric sphere illuminated by 10 plane waves, listed in Table I, versus the normalized radius r_0/λ. (a) Force component f_x as a function of r_0/λ. Gradient components f_g (dashed red curves), scattering components f_s (solid red curves), and their summations f_t (dashed green curves) based on the multipole decomposition method. The total forces of 10 independent plane waves f_s^M (blue crosses) and 10 interferential plane waves f_t^M (blue circles) based on the Mie theory. (b, c) Same as (a) except for the force components f_y and f_z.

waves f_t^M (blue circles) and the total force of 10 independent plane waves f_s^M (blue crosses) are also calculated. Considering that a single plane wave is completely attributed to the scattering force, so f_s^M is a vector summation of each single plane wave's scattering force. Perfect agreement between f_t by our approach and f_t^M by Mie theory for the total forces is reached in Figs. 3(a)–3(c). Comparing Figs. 3(a) and 3(b) with Fig. 3(c), we find the total force components f_x, f_y smaller than f_z by one order of magnitude. The gradient components of f_x and f_y approach the scattering components in Figs. 3(a) and 3(b). On the other hand, the gradient component of f_z is much smaller than the scattering component, by at least two orders of magnitude, and f_s^M approaches f_s in Fig. 3(c).

Keeping the same parameters, we explore a much larger range, $0 < r_0 < 2000\lambda$, in Fig. 4. Figures 4(a)–4(c) correspond to Figs. 3(a)–3(c) separately. It is clearly shown in Fig. 4 that the scattering forces (dotted red curves) are much larger than the gradient forces (dashed red curves) in all three directions with increasing radius. As a consequence, the total forces (dashed green curves) are dominated by the scattering forces. Meanwhile f_s^M values approach the scattering forces

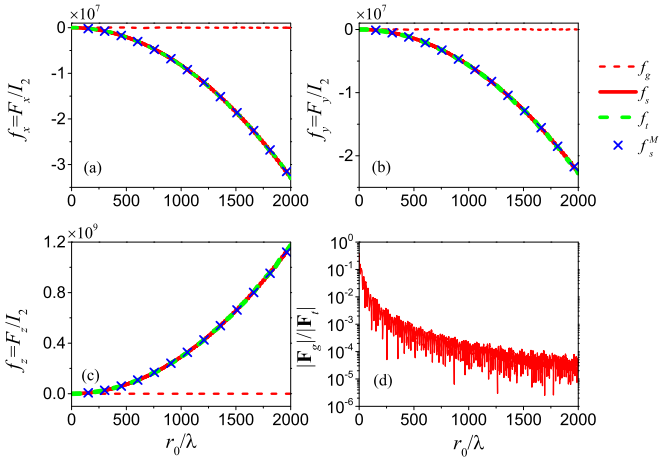

FIG. 4. (a–c) Same as Figs. 3(a)–3(c), except for the range, $0 < r_0 < 2000\lambda$. (d) Ratio of the gradient force's modulus $|\mathbf{F}_g|$ to the total force's modulus $|\mathbf{F}_t|$ on logarithmic scale.

in Figs. 4(a)–4(c). The ratio of the gradient force's modulus $|\mathbf{F}_g| = \sqrt{f_{gx}^2 + f_{gy}^2 + f_{gz}^2}$ to the total force's modulus $|\mathbf{F}_t| = \sqrt{f_{tx}^2 + f_{ty}^2 + f_{tz}^2}$ is given in Fig. 4(d) on logarithmic scale. The ratio $|\mathbf{F}_g|/|\mathbf{F}_t|$ continues to decrease with increasing radius.

We randomly choose other groups of incident plane waves with different ranges of polar angles in Fig. 5, where the sphere is fixed at origin $(0, 0, 0)$ and the ratio $|\mathbf{F}_g|/|\mathbf{F}_t|$ is depicted on logarithmic scale. The range of polar angles $0 < \alpha < 10°$, $0 < \alpha < 30°$, and $0 < \alpha < 80°$ is randomly selected for plane waves in Figs. 5(a)–5(c), 5(d)–5(f), and 5(g)–5(i), respectively. The numbers of plane waves are chosen to be 10, 50, and 100 in Figs. 5(a), 5(d), and 5(g), Figs. 5(b), 5(e), and 5(h), and Figs. 5(c), 5(f), and 5(i). With increasing radius, we find a tendency of the ratio $|\mathbf{F}_g|/|\mathbf{F}_t|$ to decrease to 0 in Figs. 5(a)–5(i), which is the same as in Fig. 4(d).

IV. CONCLUSION

We present a local decomposition scheme of the optical force into gradient and scattering components. Our approach allows for the decomposition of the optical force on a spherical particle of any size immersed in interferential optical fields made up of an arbitrary number of homogeneous plane waves. Considering that the optical beams can be depicted by an angular spectrum representation, we make use of our approach to decompose the force acting on a particle residing in a Bessel beam. Compared with the previous decomposing work based on the ray optics method, the advantage of our approach is the adaptiation of an arbitrary radius. In addition, the effect of Mie resonances on the optical force could also be observed in our approach, while they are invisible in the ray optics method. The decomposition of other optical fields, e.g., Gaussian beams and Airy beams, could be studied in the same way. The optical force acting on a spherical particle in multiple interferential plane waves with different ranges of polar angles is also decomposed, for particles of size up to 2000 wavelengths in radius. The total forces calculated by our approach are in excellent agreement with the results based on the Mie theory. Our extensive numerical results suggest an overall decreasing tendency of the ratio $|\mathbf{F}_g|/|\mathbf{F}_t|$ as the particle radius increases.

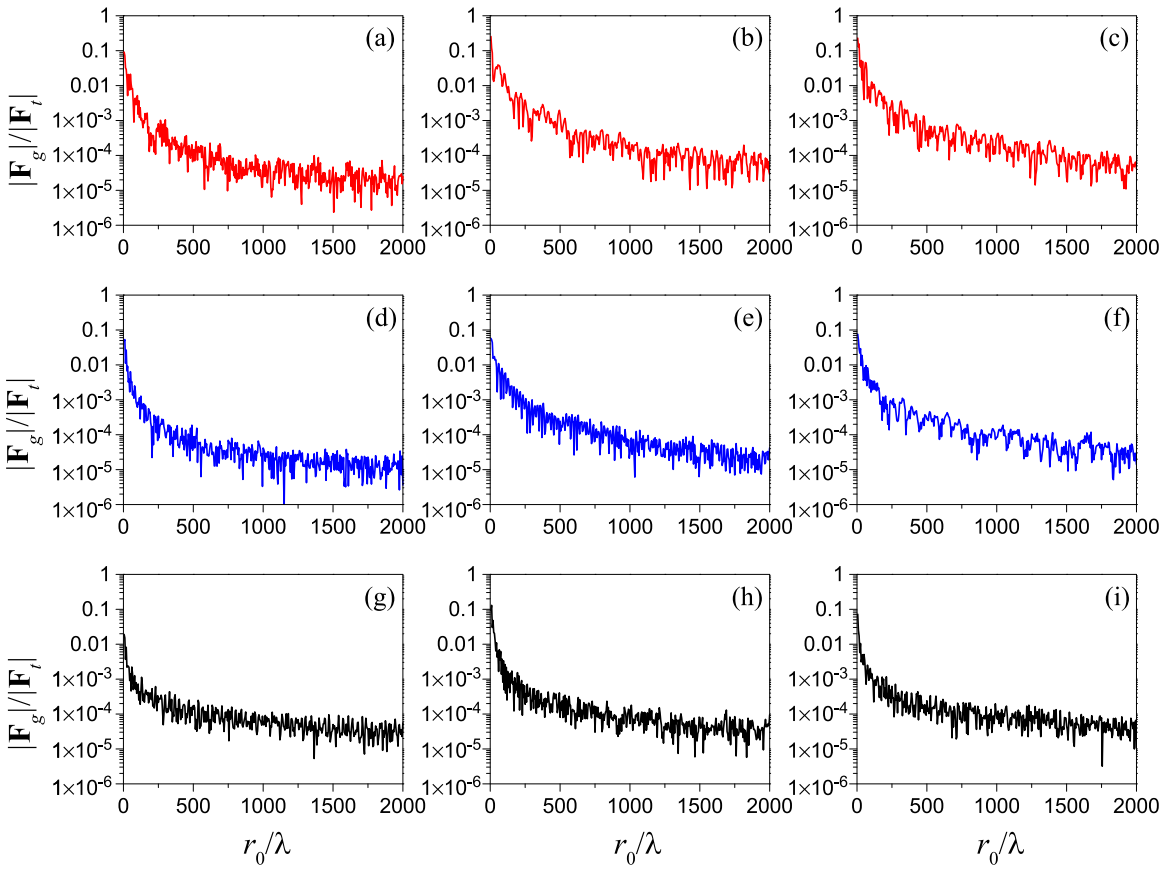

FIG. 5. Ratio of the gradient force's modulus to the total force's modulus $|\mathbf{F}_g|/|\mathbf{F}_t|$ on logarithmic scale. (a–c) Polar angles $0 < \alpha < 10°$; randomly chosen 10 plane waves (a), 50 plane waves (b), and 100 plane waves (c). (d–f) Polar angles $0 < \alpha < 30°$; randomly chosen 10 plane waves (d), 50 plane waves (e), and 100 plane waves (f). (g–i) Polar angles $0 < \alpha < 80°$; randomly chosen 10 plane waves (g), 50 plane waves (h), and 100 plane waves (i).

ACKNOWLEDGMENTS

This work was supported by the National Natural Science Foundation of China (Grants No. 11574055, No. 11804061, and No. 11574275), Zhejiang Provincial Natural Science Foundation of China (Grant No. LR16A040001), Natural Science Foundation of Guangxi Province of China (Grant No. 2018GXNSFBA281021), Open Project of State Key Laboratory of Surface Physics in Fudan University (Grant No. KF2017_4), and Research Program of Science for Universities of Guang Xi Autonomous Region (Grant No. 2018KY0328).

APPENDIX A: CARTESIAN MULTIPOLE EXPANSION THEORY

The Cartesian multipole expansion of the time-averaged optical force $\langle \mathbf{F} \rangle$ is formulated [19] based on the T-matrix method [23], the multipole field theory [35,36], the irreducible tensor theory [37], and the Maxwell stress tensor method [38,39]. Decomposition of the optical force into the gradient and scattering components on a spherical particle of arbitrary size is established on the basis of the Cartesian multipole expansion formulation [20]. Before giving the multipole expansion of the optical force, we define some field moments in reciprocal space,

$$
\begin{aligned}
D_{\mathrm{ee}}^{(n)} &= [\nabla^{(n-1)}\mathbf{E}] \overset{(n)}{\vdots} [\nabla^{(n-1)}\mathbf{E}^*], \\
D_{\mathrm{mm}}^{(n)} &= [\nabla^{(n-1)}\mathbf{B}] \overset{(n)}{\vdots} [\nabla^{(n-1)}\mathbf{B}^*], \\
\mathbf{G}_{\mathrm{ee}}^{(n)} &= [\nabla^{(n-1)}\mathbf{E}] \overset{(n)}{\vdots} [\nabla^{(n)}\mathbf{E}^*], \\
\mathbf{G}_{\mathrm{mm}}^{(n)} &= [\nabla^{(n-1)}\mathbf{B}] \overset{(n)}{\vdots} [\nabla^{(n)}\mathbf{B}^*], \\
\mathbf{G}_{\mathrm{em}}^{(n)} &= [\nabla^{(n-1)}\mathbf{E}] \overset{(n)}{\vdots} [\nabla^{(n)}\mathbf{B}^*], \\
\mathbf{G}_{\mathrm{me}}^{(n)} &= [\nabla^{(n-1)}\mathbf{B}] \overset{(n)}{\vdots} [\nabla^{(n)}\mathbf{E}^*], \\
\mathbf{S}_{\mathrm{ee}}^{(n)} &= [(\nabla^{(n-1)}\mathbf{E}) \overset{(n-1)}{\vdots} (\nabla^{(n-1)}\mathbf{E}^*)] \overset{(2)}{\vdots} \overleftrightarrow{\boldsymbol{\epsilon}}, \\
\mathbf{S}_{\mathrm{mm}}^{(n)} &= [(\nabla^{(n-1)}\mathbf{B}) \overset{(n-1)}{\vdots} (\nabla^{(n-1)}\mathbf{B}^*)] \overset{(2)}{\vdots} \overleftrightarrow{\boldsymbol{\epsilon}}, \\
\mathbf{S}_{\mathrm{em}}^{(n)} &= [(\nabla^{(n-1)}\mathbf{E}) \overset{(n-1)}{\vdots} (\nabla^{(n-1)}\mathbf{B}^*)] \overset{(2)}{\vdots} \overleftrightarrow{\boldsymbol{\epsilon}},
\end{aligned}
\tag{A1}
$$

where integers $n \geqslant 1$, $\overleftrightarrow{\boldsymbol{\epsilon}}$ is the Levi-Civita tensor, superscripts (*) denote the complex conjugates, and the tensor contraction $\overset{(n)}{\vdots}$ is defined as follows:

$$
\begin{aligned}
\overleftrightarrow{\mathbb{A}}^{(l)} \overset{(m)}{\vdots} \overleftrightarrow{\mathbb{B}}^{(l')} &= \mathbb{A}^{(l)}_{k_1 k_2 \ldots k_m i_{m+1} i_{m+2} \ldots i_l} \mathbb{B}^{(l')}_{k_1 k_2 \ldots k_m j_{m+1} j_{m+2} \ldots j_{l'}}, \\
0 &\leqslant m \leqslant \min[l, l'].
\end{aligned}
\tag{A2}
$$

In the light of the above definitions, the electric and magnetic parts of extinction forces are rewritten [20]

$$\langle \mathbf{F}_{\rm int}^{{\rm e}(l)} \rangle = \frac{1}{2\,l!} \sum_{m=0}^{\lfloor \frac{l-1}{2} \rfloor} c_{l,m} k^{4m} \,{\rm Re}\big[\gamma_{\rm elec}^{(l)}\, \mathbf{t}_{\rm elec}^{(l-2m)}\big], \quad \text{(A3a)}$$

$$\langle \mathbf{F}_{\rm int}^{{\rm m}(l)} \rangle = \frac{1}{2\,l!} \sum_{m=0}^{\lfloor \frac{l-1}{2} \rfloor} c_{l,m} k^{4m} \,{\rm Re}\big[\gamma_{\rm mag}^{(l)}\, \mathbf{t}_{\rm mag}^{(l-2m)}\big], \quad \text{(A3b)}$$

where $\lfloor x \rfloor$ gives the greatest integer less than or equal to x, and

$$\mathbf{t}_{\rm elec}^{(n)} = \mathbf{Z}_{\rm ee}^{(n)} - \frac{(n-1)\omega^2}{n}\,\mathbf{Z}_{\rm mm}^{(n-1)},$$
$$\mathbf{t}_{\rm mag}^{(n)} = \mathbf{Z}_{\rm mm}^{(n)} - \frac{(n-1)\omega^2}{n\,c^4}\,\mathbf{Z}_{\rm ee}^{(n-1)}, \quad \text{(A4)}$$

with

$$\mathbf{Z}_{\rm ee}^{(n)} \equiv \frac{1}{2}\big[\nabla D_{\rm ee}^{(n)} - \nabla\times\mathbf{S}_{\rm ee}^{(n)} - 2i\omega\,{\rm Re}\,\mathbf{S}_{\rm em}^{(n)}\big],$$
$$\mathbf{Z}_{\rm mm}^{(n)} \equiv \frac{1}{2}\left[\nabla D_{\rm mm}^{(n)} - \nabla\times\mathbf{S}_{\rm mm}^{(n)} - \frac{2i\omega}{c^2}\,{\rm Re}\,\mathbf{S}_{\rm em}^{(n)}\right]. \quad \text{(A5)}$$

The electric polarizability $\gamma_{\rm elec}^{(l)}$ and magnetic polarizability $\gamma_{\rm mag}^{(l)}$, depending on the Mie coefficients a_l and b_l [23], are expressed as

$$\gamma_{\rm elec}^{(l)} = \frac{l\,(2l+1)!}{2^l\,(l+1)!}\,\frac{4\,i\,\pi\,\varepsilon_0}{k^{2l+1}}\,a_l,$$
$$\gamma_{\rm mag}^{(l)} = \frac{l\,(2l+1)!}{2^l\,(l+1)!}\,\frac{4\,i\,\pi\,\varepsilon_0\,c^2}{k^{2l+1}}\,b_l. \quad \text{(A6)}$$

The coefficient $c_{l,m}$ is written in terms of the Gamma function $\Gamma(x)$ as

$$c_{l,m} = (-1)^m \frac{(l-2m)}{4^m l^2}\,\frac{l!}{m!}\,\frac{\Gamma\big(l-m+\frac{1}{2}\big)}{\Gamma\big(l+\frac{1}{2}\big)\,\Gamma(l-2m)}. \quad \text{(A7)}$$

In a similar way, the electric and magnetic parts of the recoil force are rewritten as

$$\langle \mathbf{F}_{\rm rec}^{{\rm e}(l)} \rangle = -\frac{c_l k^{2l+3}}{4\pi\,\varepsilon_0} \sum_{m=0}^{\lfloor \frac{l-1}{2} \rfloor} \Big\{ f_{l,m} k^{4m} {\rm Im}\big[\eta_{\rm elec}^{(l)}\, \mathbf{t}_{\rm ee}^{(l-2m)*}\big] + g_{l,m} k^{4m+2}\,{\rm Im}\big[\eta_{\rm elec}^{(l)}\, \mathbf{t}_{\rm ee}^{(l-2m-1)}\big]\Big\}, \quad \text{(A8a)}$$

$$\langle \mathbf{F}_{\rm rec}^{{\rm m}(l)} \rangle = \frac{c_l\, k^{2l+3}}{4\pi\,\varepsilon_0 c^2} \sum_{m=0}^{\lfloor \frac{l-1}{2} \rfloor} \Big\{ f_{l,m} k^{4m}\,{\rm Im}\big[\eta_{\rm mag}^{(l)}\, \mathbf{t}_{\rm mm}^{(l-2m)*}\big] + g_{l,m} k^{4m+2}\,{\rm Im}\big[\eta_{\rm mag}^{(l)}\, \mathbf{t}_{\rm mm}^{(l-2m-1)}\big]\Big\}, \quad \text{(A8b)}$$

where $c_l = 2^{l+1}(l+2)/(2l+3)!$ and

$$\mathbf{t}_{\rm ee}^{(n)} = \mathbf{Z}_{\rm ee}^{(n)} - \frac{(n-1)\omega^2}{(n+1)}\,\mathbf{Z}_{\rm mm}^{(n-1)} + \frac{i\omega}{(n+1)}\,\mathbf{S}_{\rm em}^{(n)}, \quad \text{(A9a)}$$

$$\mathbf{t}_{\rm mm}^{(n)} = \mathbf{Z}_{\rm mm}^{(n)} - \frac{(n-1)\omega^2}{(n+1)c^4}\,\mathbf{Z}_{\rm ee}^{(n-1)} + \frac{i\omega}{(n+1)c^2}\,\mathbf{S}_{\rm em}^{(n)*}. \quad \text{(A9b)}$$

Products of the polarizabilities $\eta_{\rm elec}^{(l)}$ and $\eta_{\rm mag}^{(l)}$ are proportional to the Mie coefficients $a_{l+1}a_l^*$ and $b_{l+1}b_l^*$ in GLMT,

$$\eta_{\rm elec}^{(l)} = \gamma_{\rm elec}^{(l+1)}\gamma_{\rm elec}^{(l)*}, \quad \eta_{\rm mag}^{(l)} = \gamma_{\rm mag}^{(l+1)}\gamma_{\rm mag}^{(l)*}, \quad \text{(A10)}$$

and the coefficients

$$f_{l,m} = \frac{l(l-2m+1)(2l-2m+1)}{(l+1)(2l+1)(l-2m)}c_{l,m},$$
$$g_{l,m} = \frac{l(l-2m-1)}{(l+1)(2l+1)}c_{l,m}. \quad \text{(A11)}$$

The hybrid term of the recoil force is rewritten as

$$\langle \mathbf{F}_{\rm rec}^{{\rm x}(l)} \rangle = \frac{c}{4\pi\,\varepsilon_0}\,\frac{2^l k^{2l+2}}{l\,(2l+1)!} \sum_{m=0}^{\lfloor \frac{l-1}{2} \rfloor} h_{l,m} k^{4m}\,{\rm Re}\big[\eta_{\rm hyb}^{(l)} \mathbf{t}_{\rm em}^{(l-2m)}\big], \quad \text{(A12)}$$

where

$$\mathbf{t}_{\rm em}^{(n)} = \frac{i(n-1)\omega}{n\,c^2}\big[c^2\mathbf{Z}_{\rm mm}^{(n-1)} - \mathbf{Z}_{\rm ee}^{(n-1)*}\big] + \frac{i(n-1)(n-2)\omega k^2}{n^2c^2}\big[c^2\mathbf{Z}_{\rm mm}^{(n-2)*} - \mathbf{Z}_{\rm ee}^{(n-2)}\big] - \mathbf{S}_{\rm em}^{(n)} - \frac{(n-1)k^2}{n^2}\mathbf{S}_{\rm em}^{(n-1)*} + \frac{(n-1)(n-2)k^4}{n^2}\,\mathbf{S}_{\rm em}^{(n-2)}. \quad \text{(A13)}$$

The product of polarizabilities $\eta_{\rm hyb}^{(l)}$ is proportional to the Mie coefficients $a_l b_l^*$ in GLMT. Then $\eta_{\rm hyb}^{(l)}$ and $h_{l,m}$ are written as

$$\eta_{\rm hyb}^{(l)} = \gamma_{\rm elec}^{(l)}\gamma_{\rm mag}^{(l)*}, \quad h_{l,m} = \frac{(l-2m)}{l}c_{l,m}. \quad \text{(A14)}$$

Based on the Maxwell equations, the following relations can be demonstrated,

$$\nabla D_{\rm ee}^{(n)} = 2\omega\,{\rm Im}\,\mathbf{S}_{\rm em}^{(n)} + 2\,{\rm Re}\,\mathbf{G}_{\rm ee}^{(n)},$$
$$\nabla D_{\rm mm}^{(n)} = -\frac{2\omega}{c^2}\,{\rm Im}\,\mathbf{S}_{\rm em}^{(n)} + 2\,{\rm Re}\,\mathbf{G}_{\rm mm}^{(n)}, \quad \text{(A15)}$$

which imply that $\nabla D_{\rm ee}^{(n)}$ and $\nabla D_{\rm mm}^{(n)}$ are purely real. In addition, $\nabla\times\mathbf{S}_{\rm ee}^{(n)}$ and $\nabla\times\mathbf{S}_{\rm mm}^{(n)}$ are purely imaginary and satisfy

$$\nabla\times\mathbf{S}_{\rm ee}^{(n)} = -2i\,{\rm Im}\,\mathbf{G}_{\rm ee}^{(n)}, \quad \nabla\times\mathbf{S}_{\rm mm}^{(n)} = -2i\,{\rm Im}\,\mathbf{G}_{\rm mm}^{(n)}. \quad \text{(A16)}$$

As a consequence, the complex vectors $\mathbf{Z}_{\rm ee}^{(n)}$ and $\mathbf{Z}_{\rm mm}^{(n)}$ in Eqs. (A5) are decomposed into an irrotational part (denoted by the superscript "grad") and a solenoidal part (denoted by the superscript "curl"),

$$\mathbf{Z}_{\rm ee}^{(n){\rm grad}} = {\rm Re}\,\mathbf{Z}_{\rm ee}^{(n)} = \frac{1}{2}\nabla D_{\rm ee}^{(n)},$$
$$\mathbf{Z}_{\rm ee}^{(n){\rm curl}} = i{\rm Im}\,\mathbf{Z}_{\rm ee}^{(n)} = -\frac{1}{2}\nabla\times\mathbf{S}_{\rm ee}^{(n)} - i\omega\,{\rm Re}\,\mathbf{S}_{\rm em}^{(n)},$$
$$\mathbf{Z}_{\rm mm}^{(n){\rm grad}} = {\rm Re}\,\mathbf{Z}_{\rm mm}^{(n)} = \frac{1}{2}\nabla D_{\rm mm}^{(n)},$$
$$\mathbf{Z}_{\rm mm}^{(n){\rm curl}} = i{\rm Im}\,\mathbf{Z}_{\rm mm}^{(n)} = -\frac{1}{2}\nabla\times\mathbf{S}_{\rm mm}^{(n)} - \frac{i\omega}{c^2}\,{\rm Re}\,\mathbf{S}_{\rm em}^{(n)}, \quad \text{(A17)}$$

where $\mathbf{S}_{\rm em}^{(n)}$ is derived as

$$\mathbf{S}_{\rm em}^{(n)} = -\frac{i}{2\omega}\nabla\sum_{m=0}^{\infty}\frac{1}{k^{2m}}\left[c^2 D_{\rm mm}^{(n+m)} - D_{\rm ee}^{(n+m)}\right] - \frac{1}{2k^2}\nabla\times\sum_{m=0}^{\infty}\frac{1}{k^{2m}}\left[\mathbf{G}_{\rm em}^{(n+m)} - \mathbf{G}_{\rm me}^{(n+m)*}\right] + \mathbf{P}^{(n)}. \tag{A18}$$

The spatially constant real vector $\mathbf{P}^{(n)}$ is a missed term in the decomposition of $\mathbf{S}_{\rm em}^{(n)}$ by Helmholtz's theorem [22]. $\mathbf{P}^{(n)}$ can be regarded as the irrotational part, the solenoidal part, or their linear combination. In our treatment, $\mathbf{P}^{(n)}$ is completely solenoidal so that the force acting on a sphere immersed in a homogeneous plane wave is regarded as the scattering force, and then

$$\mathrm{Re}\,\mathbf{S}_{\rm em}^{(n)} = -\frac{1}{2k^2}\nabla\times\sum_{m=0}^{\infty}\frac{1}{k^{2m}}\mathrm{Re}\left[\mathbf{G}_{\rm em}^{(n+m)} - \mathbf{G}_{\rm me}^{(n+m)*}\right] + \mathbf{P}^{(n)} \tag{A19}$$

is solenoidal, i.e., $\nabla\cdot\mathrm{Re}\,\mathbf{S}_{\rm em}^{(n)} = 0$. Meanwhile, the imaginary part of $\mathbf{S}_{\rm em}^{(n)}$ is divided:

$$\mathrm{Im}\mathbf{S}_{\rm em}^{(n)\rm grad} = -\frac{1}{2\omega}\nabla\sum_{m=0}^{\infty}\frac{1}{k^{2m}}\left[c^2 D_{\rm mm}^{(n+m)} - D_{\rm ee}^{(n+m)}\right], \tag{A20a}$$

$$\mathrm{Im}\mathbf{S}_{\rm em}^{(n)\rm curl} = -\frac{1}{2k^2}\nabla\times\sum_{m=0}^{\infty}\frac{1}{k^{2m}}\mathrm{Im}\left[\mathbf{G}_{\rm em}^{(n+m)} - \mathbf{G}_{\rm me}^{(n+m)*}\right]. \tag{A20b}$$

Extinction and recoil forces consist of $\mathbf{Z}_{\rm ee}^{(n)}$, $\mathbf{Z}_{\rm mm}^{(n)}$, $\mathbf{S}_{\rm em}^{(n)}$, and their complex conjugates in Eqs. (A4), (A9), and (A13). So the total forces are decomposed into gradient and scattering parts.

APPENDIX B: OPTICAL FIELD COMPOSED OF MULTIPLE PLANE WAVES

In this section, we work out the extinction and recoil forces of an arbitrary superposition of homogeneous plane waves in terms of Legendre polynomials. In order to get the dimensionless force, we set the parameters $k = \omega = c = 1$. Substituting Eqs. (A4), (A6), and (6) into Eqs. (A3) yields

$$\left\langle\mathbf{F}_{\rm int}^{{\rm e}(l)}\right\rangle = -\frac{2\pi\varepsilon_0 l(2l+1)!}{2^l(l+1)!}\mathrm{Im}\sum_{i,\,j}a_l\,\mathbf{T}_{{\rm i},ij}^{{\rm e}(l)}, \quad \left\langle\mathbf{F}_{\rm int}^{{\rm m}(l)}\right\rangle = -\frac{2\pi\varepsilon_0 l(2l+1)!}{2^l(l+1)!}\mathrm{Im}\sum_{i,\,j}b_l\,\mathbf{T}_{{\rm i},ij}^{{\rm m}(l)}, \tag{B1}$$

with

$$\mathbf{T}_{{\rm i},ij}^{{\rm e}(l)} = \mathbf{Z}_{{\rm ee},ij}^{(1)}\sum_{m=0}^{\lfloor\frac{l-1}{2}\rfloor}c_{l,m}x_{ij}^{l-2m-1} - \mathbf{Z}_{{\rm mm},ij}^{(1)}\sum_{m=0}^{\lfloor\frac{l-1}{2}\rfloor}\frac{l-2m-1}{l-2m}c_{l,m}x_{ij}^{l-2m-2},$$
$$\mathbf{T}_{{\rm i},ij}^{{\rm m}(l)} = \mathbf{Z}_{{\rm mm},ij}^{(1)}\sum_{m=0}^{\lfloor\frac{l-1}{2}\rfloor}c_{l,m}x_{ij}^{l-2m-1} - \mathbf{Z}_{{\rm ee},ij}^{(1)}\sum_{m=0}^{\lfloor\frac{l-1}{2}\rfloor}\frac{l-2m-1}{l-2m}c_{l,m}x_{ij}^{l-2m-2}. \tag{B2}$$

Equations (B1) are the extinction forces of n_p plane waves. Similarly, substituting Eqs. (A4), (A10), and (6) into Eqs. (A8), the electric and magnetic parts of the recoil force are obtained,

$$\left\langle\mathbf{F}_{\rm rec}^{{\rm e}(l)}\right\rangle = -\frac{4\pi\varepsilon_0(2l+1)!}{2^l(l+1)!(l-1)!}\mathrm{Im}\sum_{i,\,j}a_{l+1}a_l^*\left[\mathbf{T}_{{\rm r1},ij}^{{\rm e}(l)} + \mathbf{T}_{{\rm r2},ij}^{{\rm e}(l)} + \mathbf{T}_{{\rm r3},ij}^{{\rm e}(l)}\right],$$
$$\left\langle\mathbf{F}_{\rm rec}^{{\rm m}(l)}\right\rangle = -\frac{4\pi\varepsilon_0(2l+1)!}{2^l(l+1)!(l-1)!}\mathrm{Im}\sum_{i,\,j}b_{l+1}b_l^*\left[\mathbf{T}_{{\rm r1},ij}^{{\rm m}(l)} + \mathbf{T}_{{\rm r2},ij}^{{\rm m}(l)} + \mathbf{T}_{{\rm r3},ij}^{{\rm m}(l)}\right], \tag{B3}$$

where

$$\mathbf{T}_{{\rm r1},ij}^{{\rm e}(l)} = \mathbf{Z}_{{\rm ee},ij}^{(1)*}\sum_{m=0}^{\lfloor\frac{l-1}{2}\rfloor}f_{l,m}x_{ij}^{l-2m-1} - \mathbf{Z}_{{\rm mm},ij}^{(1)*}\sum_{m=0}^{\lfloor\frac{l-1}{2}\rfloor}\frac{l-2m-1}{l-2m+1}f_{l,m}x_{ij}^{l-2m-2},$$
$$\mathbf{T}_{{\rm r2},ij}^{{\rm e}(l)} = \mathbf{Z}_{{\rm ee},ij}^{(1)}\sum_{m=0}^{\lfloor\frac{l-1}{2}\rfloor}g_{l,m}x_{ij}^{l-2m-2} - \mathbf{Z}_{{\rm mm},ij}^{(1)}\sum_{m=0}^{\lfloor\frac{l-1}{2}\rfloor}\frac{l-2m-2}{l-2m}g_{l,m}x_{ij}^{l-2m-3},$$
$$\mathbf{T}_{{\rm r3},ij}^{{\rm e}(l)} = -i\mathbf{S}_{{\rm em},ij}^{(1)*}\sum_{m=0}^{\lfloor\frac{l-1}{2}\rfloor}\frac{f_{l,m}x_{ij}^{l-2m-1}}{l-2m+1} + i\mathbf{S}_{{\rm em},ij}^{(1)}\sum_{m=0}^{\lfloor\frac{l-1}{2}\rfloor}\frac{g_{l,m}x_{ij}^{l-2m-2}}{l-2m} \tag{B4}$$

and

$$\mathbf{T}^{\mathrm{m}(l)}_{\mathrm{r1},ij} = \mathbf{Z}^{(1)*}_{\mathrm{mm},ij}\sum_{m=0}^{\lfloor\frac{l-1}{2}\rfloor} f_{l,m}x_{ij}^{l-2m-1} - \mathbf{Z}^{(1)*}_{\mathrm{ee},ij}\sum_{m=0}^{\lfloor\frac{l-1}{2}\rfloor}\frac{l-2m-1}{l-2m+1}f_{l,m}x_{ij}^{l-2m-2},$$

$$\mathbf{T}^{\mathrm{m}(l)}_{\mathrm{r2},ij} = \mathbf{Z}^{(1)}_{\mathrm{mm},ij}\sum_{m=0}^{\lfloor\frac{l-1}{2}\rfloor} g_{l,m}x_{ij}^{l-2m-2} - \mathbf{Z}^{(1)}_{\mathrm{ee},ij}\sum_{m=0}^{\lfloor\frac{l-1}{2}\rfloor}\frac{l-2m-2}{l-2m}g_{l,m}x_{ij}^{l-2m-3},$$

$$\mathbf{T}^{\mathrm{m}(l)}_{\mathrm{r3},ij} = -i\mathbf{S}^{(1)}_{\mathrm{em},ij}\sum_{m=0}^{\lfloor\frac{l-1}{2}\rfloor}\frac{f_{l,m}x_{ij}^{l-2m-1}}{l-2m+1} + i\mathbf{S}^{(1)*}_{\mathrm{em},ij}\sum_{m=0}^{\lfloor\frac{l-1}{2}\rfloor}\frac{g_{l,m}x_{ij}^{l-2m-2}}{l-2m}. \tag{B5}$$

Substituting Eqs. (A4), (A14), and (6) into Eq. (A12), the hybrid part of the recoil force is obtained,

$$\left\langle\mathbf{F}^{\mathrm{x}(l)}_{\mathrm{rec}}\right\rangle = -\frac{4\pi\varepsilon_0 l(2l+1)!}{2^l(l+1)!(l+1)!}\mathrm{Im}\sum_{i,\,j} a_l b_l^*\left[\mathbf{T}^{\mathrm{x}(l)}_{\mathrm{r1},ij} + \mathbf{T}^{\mathrm{x}(l)}_{\mathrm{r2},ij} + \mathbf{T}^{\mathrm{x}(l)}_{\mathrm{r3},ij} + \mathbf{T}^{\mathrm{x}(l)}_{\mathrm{r4},ij}\right], \tag{B6}$$

with

$$\mathbf{T}^{\mathrm{x}(l)}_{\mathrm{r1},ij} = \left[\mathbf{Z}^{(1)}_{\mathrm{mm},ij} - \mathbf{Z}^{(1)*}_{\mathrm{ee},ij}\right]\sum_{m=0}^{\lfloor\frac{l-1}{2}\rfloor}\frac{l-2m-1}{l-2m}h_{l,m}x_{ij}^{l-2m-2},$$

$$\mathbf{T}^{\mathrm{x}(l)}_{\mathrm{r2},ij} = \left[\mathbf{Z}^{(1)*}_{\mathrm{mm},ij} - \mathbf{Z}^{(1)}_{\mathrm{ee},ij}\right]\sum_{m=0}^{\lfloor\frac{l-1}{2}\rfloor}\frac{(l-2m-1)(l-2m-2)}{(l-2m)^2}h_{l,m}x_{ij}^{l-2m-3},$$

$$\mathbf{T}^{\mathrm{x}(l)}_{\mathrm{r3},ij} = i\mathbf{S}^{(1)}_{\mathrm{em},ij}\sum_{m=0}^{\lfloor\frac{l-1}{2}\rfloor}\left[h_{l,m}x_{ij}^{l-2m-1} - \frac{(l-2m-1)(l-2m-2)}{(l-2m)^2}h_{l,m}x_{ij}^{l-2m-3}\right],$$

$$\mathbf{T}^{\mathrm{x}(l)}_{\mathrm{r4},ij} = i\mathbf{S}^{(1)*}_{\mathrm{em},ij}\sum_{m=0}^{\lfloor\frac{l-1}{2}\rfloor}\frac{(l-2m-1)}{(l-2m)^2}h_{l,m}x_{ij}^{l-2m-2}. \tag{B7}$$

It is noted that l runs from 1 to n_c and the empirical formula for the cutoff coefficient n_c is [40]

$$n_c = x + 4.05x^{1/3} + 2, \tag{B8}$$

where x is the particle's size parameter. Nevertheless, the summations involving $c_{l,m}$, $f_{l,m}$, $g_{l,m}$, and $h_{l,m}$ in Eqs. (B1)–(B7) would be numerically inaccurate along with the increasing orders l. This is due to roundoff error resulting from cancellation of terms in summations of approximately equal magnitudes and opposite signs. Making use of the completeness properties of Legendre polynomials, the relationships between the Legendre polynomials and summations of $c_{l,m}$, $f_{l,m}$, $g_{l,m}$, and $h_{l,m}$ over m in Eqs. (B1)–(B7) could be demonstrated by mathematical induction,

$$\sum_{m=0}^{\lfloor\frac{l-1}{2}\rfloor} c_{l,m}x_{ij}^{l-2m-1} = s_l^{(1)}Q_{l,ij}^{(1)}, \quad \sum_{m=0}^{\lfloor\frac{l-1}{2}\rfloor}\frac{l-2m-1}{l-2m}c_{l,m}x_{ij}^{l-2m-2} = s_l^{(1)}Q_{l,ij}^{(2)}, \tag{B9a}$$

$$\sum_{m=0}^{\lfloor\frac{l-1}{2}\rfloor} f_{l,m}x_{ij}^{l-2m-1} = s_l^{(2)}R_{l,ij}^{(1)}, \quad \sum_{m=0}^{\lfloor\frac{l-1}{2}\rfloor}\frac{l-2m-1}{l-2m+1}f_{l,m}x_{ij}^{l-2m-2} = s_l^{(2)}R_{l,ij}^{(2)}, \tag{B9b}$$

$$\sum_{m=0}^{\lfloor\frac{l-1}{2}\rfloor}\frac{f_{l,m}x_{ij}^{l-2m-1}}{l-2m+1} = 4s_l^{(2)}R_{l,ij}^{(3)}, \quad \sum_{m=0}^{\lfloor\frac{l-1}{2}\rfloor}\frac{l-2m-2}{l-2m}g_{l,m}x_{ij}^{l-2m-3} = s_l^{(2)}R_{l,ij}^{(5)}, \tag{B9c}$$

$$\sum_{m=0}^{\lfloor\frac{l-1}{2}\rfloor} g_{l,m}x_{ij}^{l-2m-2} = s_l^{(2)}R_{l,ij}^{(4)}, \quad \sum_{m=0}^{\lfloor\frac{l-1}{2}\rfloor}\frac{g_{l,m}x_{ij}^{l-2m-2}}{l-2m} = 4s_l^{(2)}R_{l,ij}^{(6)}, \tag{B9d}$$

$$\sum_{m=0}^{\lfloor\frac{l-1}{2}\rfloor}\frac{l-2m-1}{l-2m}h_{l,m}x_{ij}^{l-2m-2} = s_l^{(3)}R_{l,ij}^{(4)}, \quad \sum_{m=0}^{\lfloor\frac{l-1}{2}\rfloor} h_{l,m}x_{ij}^{l-2m-1} = s_l^{(3)}\left[R_{l,ij}^{(5)} + 4R_{l,ij}^{(7)}\right], \tag{B9e}$$

$$\sum_{m=0}^{\lfloor\frac{l-1}{2}\rfloor}\frac{(l-2m-1)(l-2m-2)}{(l-2m)^2}h_{l,m}x_{ij}^{l-2m-3}=s_l^{(3)}R_{l,ij}^{(5)}, \tag{B9f}$$

$$\sum_{m=0}^{\lfloor\frac{l-1}{2}\rfloor}\frac{(l-2m-1)}{(l-2m)^2}h_{l,m}x_{ij}^{l-2m-2}=4s_l^{(3)}R_{l,ij}^{(6)}, \tag{B9g}$$

where the coefficients

$$s_l^{(1)}=\frac{2l+1}{2l(l+1)}\frac{2^l l!(l+1)!}{l(2l+1)!},\quad s_l^{(2)}=\frac{2^{l-3}(l+1)!(l-1)!}{(l+1)^2(2l+1)!},\quad s_l^{(3)}=\frac{1}{4l}s_l^{(1)}. \tag{B10}$$

Substituting Eqs. (B9a) into Eqs. (B2), extinction forces are simplified to the following expressions:

$$\langle\mathbf{F}_{\rm int}^{{\rm e}(l)}\rangle=u_l^{(1)}{\rm Im}\sum_{i,j}a_l\big[Q_{l,ij}^{(1)}\mathbf{Z}_{{\rm ee},ij}^{(1)}-Q_{l,ij}^{(2)}\mathbf{Z}_{{\rm mm},ij}^{(1)}\big], \tag{B11a}$$

$$\langle\mathbf{F}_{\rm int}^{{\rm m}(l)}\rangle=u_l^{(1)}{\rm Im}\sum_{i,j}b_l\big[Q_{l,ij}^{(1)}\mathbf{Z}_{{\rm mm},ij}^{(1)}-Q_{l,ij}^{(2)}\mathbf{Z}_{{\rm ee},ij}^{(1)}\big]. \tag{B11b}$$

Analogously, substituting Eqs. (B9b)–(B9d) into Eqs. (B4) and (B5), and substituting Eqs. (B9e)–(B9g) into Eqs. (B7), recoil forces in terms of Legendre polynomials could be obtained,

$$\langle\mathbf{F}_{\rm rec}^{{\rm e}(l)}\rangle=u_l^{(2)}{\rm Im}\sum_{i,j}a_{l+1}a_l^*\big[R_{l,ij}^{(1)}\mathbf{Z}_{{\rm ee},ij}^{(1)*}-R_{l,ij}^{(2)}\mathbf{Z}_{{\rm mm},ij}^{(1)*}-4iR_{l,ij}^{(3)}\mathbf{S}_{{\rm em},ij}^{(1)*}+R_{l,ij}^{(4)}\mathbf{Z}_{{\rm ee},ij}^{(1)}-R_{l,ij}^{(5)}\mathbf{Z}_{{\rm mm},ij}^{(1)}+4iR_{l,ij}^{(6)}\mathbf{S}_{{\rm em},ij}^{(1)}\big], \tag{B12a}$$

$$\langle\mathbf{F}_{\rm rec}^{{\rm m}(l)}\rangle=u_l^{(2)}{\rm Im}\sum_{i,j}b_{l+1}b_l^*\big[R_{l,ij}^{(1)}\mathbf{Z}_{{\rm mm},ij}^{(1)*}-R_{l,ij}^{(2)}\mathbf{Z}_{{\rm ee},ij}^{(1)*}-4iR_{l,ij}^{(3)}\mathbf{S}_{{\rm em},ij}^{(1)}+R_{l,ij}^{(4)}\mathbf{Z}_{{\rm mm},ij}^{(1)}-R_{l,ij}^{(5)}\mathbf{Z}_{{\rm ee},ij}^{(1)}+4iR_{l,ij}^{(6)}\mathbf{S}_{{\rm em},ij}^{(1)*}\big], \tag{B12b}$$

$$\langle\mathbf{F}_{\rm rec}^{{\rm x}(l)}\rangle=u_l^{(3)}{\rm Im}\sum_{i,j}a_lb_l^*\big[R_{l,ij}^{(4)}\big(\mathbf{Z}_{{\rm mm},ij}^{(1)}-\mathbf{Z}_{{\rm ee},ij}^{(1)*}\big)+R_{l,ij}^{(5)}\big(\mathbf{Z}_{{\rm mm},ij}^{(1)*}-\mathbf{Z}_{{\rm ee},ij}^{(1)}\big)+4iR_{l,ij}^{(6)}\mathbf{S}_{{\rm em},ij}^{(1)*}+4iR_{l,ij}^{(7)}\mathbf{S}_{{\rm em},ij}^{(1)}\big], \tag{B12c}$$

with

$$u_l^{(1)}=-\frac{\pi\varepsilon_0(2l+1)}{l(l+1)},\quad u_l^{(2)}=-\frac{\pi\varepsilon_0}{2(l+1)^2},\quad u_l^{(3)}=-\frac{\pi\varepsilon_0(2l+1)}{2l^2(l+1)^2}. \tag{B13}$$

The extinction and recoil forces in Eqs. (B11) and (B12) are completely in terms of Legendre polynomials, which could avoid the numerical instability for large orders l in Eqs. (B1)–(B7).

[1] A. Ashkin, Acceleration and Trapping of Particles by Radiation Pressure, Phys. Rev. Lett. **24**, 156 (1970).

[2] A. Ashkin, J. M. Dziedzic, J. E. Bjorkholm, and S. Chu, Observation of a single-beam gradient force optical trap for dielectric particles, Opt. Lett. **11**, 288 (1986).

[3] A. Ashkin and J. Dziedzic, Optical trapping and manipulation of viruses and bacteria, Science **235**, 1517 (1987).

[4] A. Ashkin, J. M. Dziedzic, and T. Yamane, Optical trapping and manipulation of single cells using infrared laser beams, Nature **330**, 769 (1987).

[5] S. Chu, The manipulation of neutral particles, Rev. Mod. Phys. **70**, 685 (1998).

[6] D. G. Grier, A revolution in optical manipulation, Nature **424**, 810 (2003).

[7] A. Ashkin and J. P. Gordon, Stability of radiation-pressure particle traps: An optical Earnshaw theorem, Opt. Lett. **8**, 511 (1983).

[8] A. Ashkin, Forces of a single-beam gradient laser trap on a dielectric sphere in the ray optics regime, Biophys. J. **61**, 569 (1992).

[9] S. Earnshaw, On the nature of the molecular forces which regulate the constitution of the luminiferous ether, Trans. Cambridge Philos. Soc. **7**, 97 (1842).

[10] C. H. Papas, On the contactless suspension of objects by electric and magnetic fields, Appl. Phys. **13**, 361 (1977).

[11] M. V. Berry and P. Shukla, Physical curl forces: Dipole dynamics near optical vortices, J. Phys. A: Math. Theor. **46**, 422001 (2013).

[12] J. P. Gordon, Radiation forces and momenta in dielectric media, Phys. Rev. A **8**, 14 (1973).

[13] G. Roosen and C. Imbert, Optical levitation by means of two horizontal laser beams: A theoretical and experimental study, Phys. Lett. A **59**, 6 (1976).

[14] G. Gouesbet and G. Gréhan, *Generalized Lorenz-Mie Theories*, 2nd ed. (Springer, Berlin, 2017).

[15] G. Gouesbet, Generalized Lorenz–Mie theories and mechanical effects of laser light, on the occasion of Arthur Ashkin's receipt of the 2018 Nobel rize in physics for his pioneering work in optical levitation and manipulation: A review, J. Quantum Spectrosc. Radiat. Transf. **225**, 258 (2019).

[16] J. P. Barton, D. R. Alexander, and S. A. Schaub, Theoretical determination of net radiation force and torque for a spherical particle illuminated by a focused laser beam, J. Appl. Phys. **66**, 4594 (1989).

[17] J. J. Du, C.-H. Yuen, X. Li, K. Ding, G. Q. Du, Z. F. Lin, C. T. Chan, and J. Ng, Tailoring optical gradient force and optical scattering and absorption force, Sci. Rep. **7**, 18042 (2017).

[18] H. X. Zheng, X. N. Yu, W. L. Lu, J. Ng, and Z. F. Lin, Gcforce: Decomposition of optical force into gradient and scattering parts, Comput. Phys. Commun. **237**, 188 (2019).

[19] Y. Jiang, H. Chen, J. Chen, J. Ng, and Z. Lin, Universal relationships between optical force/torque and orbital versus spin momentum/angular momentum of light, arXiv:1511.08546.

[20] Y. Jiang, J. Chen, J. Ng, and Z. Lin, Decomposition of optical force into conservative and nonconservative components, arXiv:1604.05138.

[21] L. Novotny and B. Hecht, *Principles of Nano-Optics*, 2nd ed. (Cambridge University Press, Cambridge, UK, 2012).

[22] R. Baierlein, Representing a vector field: Helmholtz's theorem derived from a Fourier identity, Am. J. Phys. **63**, 180 (1995).

[23] C. F. Bohren and D. R. Huffman, *Absorption and Scattering of Light by Small Particles* (John Wiley & Sons, New York, 1983).

[24] Y. Jiang, H. Lin, X. Li, J. Chen, and J. Ng, Hidden symmetry and invariance in optical force (unpublished).

[25] Z. Bouchal and M. Olivík, Non-diffractive vector Bessel beams, J. Mod. Opt. **42**, 1555 (1995).

[26] J. Chen, J. Ng, P. Wang, and Z. F. Lin, Analytical partial wave expansion of vector Bessel beam and its application to optical binding, Opt. Lett. **35**, 1674 (2010).

[27] N. Wang, J. Chen, S. Y. Liu, and Z. F. Lin, Dynamical and phase-diagram study on stable optical pulling force in Bessel beams, Phys. Rev. A **87**, 063812 (2013).

[28] R. Piessens and M. Branders, A note on the optimal addition of abscissas to quadrature formulas of Gauss and Lobatto type, Math. Comput. **28**, 135 (1974).

[29] S. Ehrich, Stopping functionals for Gaussian quadrature formulas, J. Comput. Appl. Math. **127**, 153 (2001).

[30] S. K. Song, N. Wang, W. L. Lu, and Z. F. Lin, Optical force on a large sphere illuminated by Bessel beams: Comparisons between ray optics method and generalized Lorenz-Mie theory, J. Opt. Soc. Am. A **31**, 2192 (2014).

[31] H. C. van de Hulst, *Light Scattering by Small Particles* (Dover, Mineola, NY, 1981).

[32] J. Ng, C. T. Chan, P. Sheng, and Z. F. Lin, Strong optical force induced by morphology-dependent resonances, Opt. Lett. **30**, 1956 (2005).

[33] J. J. Du, Z. F. Lin, S. T. Chui, W. L. Lu, H. Li, A. M. Wu, Z. Sheng, J. Zi, X. Wang, S. C. Zou, and F. W. Gan, Optical Beam Steering Based on the Symmetry of Resonant Modes of Nanoparticles, Phys. Rev. Lett. **106**, 203903 (2011).

[34] X. N. Yu, Q. Ye, H. J. Chen, S. Y. Liu, and Z. F. Lin, Simple algorithm for partial wave expansion of plasmonic and evanescent fields, Opt. Express **25**, 4201 (2017).

[35] J. A. Stratton, *Electromagnetic Theory* (McGraw–Hill, New York, 1941).

[36] M. E. Rose, *Multipole Fields* (John Wiley & Sons, New York, 1951).

[37] B. L. Silver, *Irreducible Tensor Methods* (Academic Press, New York, 1976).

[38] J. D. Jackson, *Classical Electrodynamics*, 3rd ed. (John Wiley & Sons, New York, 1999).

[39] Q. Ye and H. Z. Lin, On deriving the Maxwell stress tensor method for calculating the optical force and torque on an object in harmonic electromagnetic fields, Eur. J. Phys. **38**, 045202 (2017).

[40] W. J. Wiscombe, Improved Mie scattering algorithms, Appl. Opt. **19**, 1505 (1980).